

# Structural transformations in overlayer and sticking probability during chemisorption: oxygen on (100) surface of metals

A.N. Salanov<sup>\*</sup>, V.N. Bibin, V.T. Yakushko

*Boreskov Institute of Catalysis, Prospekt Akademika Lavrentieva 5, Novosibirsk 630090, Russia*

## Abstract

The effect of the formation of  $p(2 \times 2)$  and  $c(2 \times 2)$  adsorption structures on the  $O_2$  sticking probability was studied by the Monte Carlo simulation of the  $O_2$  chemisorption on a (100) metal surface. The model used in the simulation took into account the direct and indirect adsorption pathways and repulsive lateral interactions in the adsorption layer. The ratio between the activation energy of adsorption via the direct and indirect pathways ( $E_{dir}/E_{indir}$ ) determines the character of the structural transformations in the adsorption layer, which in turn determines the type of the  $S(\theta)$  dependence. At  $E_{dir}/E_{indir} < 7-8$ , the direct pathway predominates over the indirect one. In this case, a lot of small adsorption islands nucleate to form a disordered  $p(2 \times 2)$  and  $c(2 \times 2)$  adsorption layers, i.e. Langmuir adsorption is observed, and  $S$  smoothly decreases with the  $\theta$  growth. At  $E_{dir}/E_{indir} > 7-8$ , the indirect pathway predominates over the direct one. In this case, after slow nucleation, the adsorption islands grow quickly to form ordered  $p(2 \times 2)$  and  $c(2 \times 2)$  adsorption layers, i.e. the island-mediated adsorption is observed and  $S(\theta)$  dependence passes over a maximum. © 2000 Elsevier Science B.V. All rights reserved.

*Keywords:* Computer simulations; Chemisorption; Oxygen; Sticking probability; Surface Structures

## 1. Introduction

The character of the dependence of the gas sticking probability ( $S$ ) on the adsorbate surface coverage ( $\theta$ ) can reveal the role of different factors in the chemisorption, i.e. the chemisorption mechanism [1]. Such relations as  $S \sim (1 - \theta)$  and  $S \sim (1 - \theta)^2$  correspond to the ideal Langmuir adsorption. A constant  $S$  value at the beginning of adsorption is usually related to the precursor-mediated adsorption. Curves  $S \sim$

$\exp(-\alpha\theta)$  may indicate the presence of surface adsorption sites with different activity or lateral interactions in the adsorption layer,  $S(\theta)$  dependence having a maximum usually corresponding to the island-mediated adsorption. At relatively low temperatures ( $\leq 500-700$  K), when the diffusion of chemisorbed particles on the surface is limited, various adsorption structures are formed during the chemisorption on metal monocrystals due to the lateral interactions in the adsorption layer [2]. For example, simple  $p(2 \times 2)$  and  $c(2 \times 2)$  adsorption structures are formed via the island-mediated mechanism during the  $O_2$  chemisorption on Pd(100) [3–7],

<sup>\*</sup> Corresponding author. Fax: +7-383-234-3056.  
E-mail address: salanov@catalysis.nsk.su (A.N. Salanov).

Rh(100) [8–11] and Ni(100) [12,13] at  $100 \text{ K} \leq T \leq 400 \text{ K}$  and  $\theta \leq 0.5$ . At the beginning of the chemisorption at  $\theta \leq 0.05$ – $0.1$ , islands with  $p(2 \times 2)$  structure are formed. At  $\theta = 0.2$ – $0.25$ , they merge into a saturated adsorption layer where islands with the  $c(2 \times 2)$  structure are nucleated. The latter also gradually grow to merge into a saturated adsorption layer with the  $c(2 \times 2)$  structure at  $\theta \geq 0.4$ . In our previous works [14–16], the mechanisms of the formation of the adsorption islands with  $(1 \times 1)$  [14,15],  $p(2 \times 2)$  and  $c(2 \times 2)$  structures [16] during the  $\text{O}_2$  chemisorption on a square lattice have been studied by the Monte Carlo method. In the present work, the effect of the formation of  $p(2 \times 2)$  and  $c(2 \times 2)$  adsorption structures on the character of the dependence of  $\text{O}_2$  sticking probability on the surface coverage during  $\text{O}_2$  chemisorption on a (100) surface has been studied. With this purpose, an analysis of the simulation results of the  $\text{O}_2$  chemisorption on a (100) metal surface obtained by the Monte Carlo method has been performed.

## 2. Chemisorption model

The chemisorption model, which took into account the direct and indirect adsorption pathways and repulsive lateral interactions between chemisorbed particles, was used [16]. Direct chemisorption is observed when molecules chemisorb immediately after collision with the surface. Indirect chemisorption is observed when after collision with the surface, molecules become trapped into a precursor, migrate over the surface, and finally, chemisorb (precursor-mediated chemisorption) [17]. The simple pair-wise  $\varepsilon_1$ ,  $\varepsilon_2$ , and  $\varepsilon_3$  interactions between chemisorbed oxygen atoms located in the nearest neighbor (NN), next-nearest neighbor (2NN) and third-nearest neighbor (3NN) adsorption sites, respectively, are considered in the adsorption oxygen layer on a metal surface with a square lattice of adsorption sites [13,18,19]. The  $\varepsilon_1$  repulsion is too strong. Therefore, chemisorbed

oxygen atoms are not located on the nearest NN adsorption sites. The  $\varepsilon_3$  attractive interaction is too weak, and was not taken into account. The  $\varepsilon_2$  repulsion between two oxygen atoms chemisorbed on adjacent 2NN sites decreases the adsorption heat  $\Delta q = -\varepsilon_2$ , and correspondingly increases the activation energy of adsorption according to Temkin relation between the change of the heat and activation energy of chemisorption  $\Delta E = -\alpha \Delta q$  ( $0 < \alpha < 1$ ) [20,21]. Thus, an  $\text{O}_2$  molecule can dissociatively chemisorb on 3NN adsorption sites due to strong  $\varepsilon_1$  repulsion and weaker  $\varepsilon_3$  attraction between the chemisorbed atoms with the probability  $W_a = \exp(-(E_{\text{dir,indir}} + N\Delta E)/RT)$ , where  $E_{\text{dir,indir}}$  is the activation energy of the  $\text{O}_2$  dissociative chemisorption on 3NN sites when all adjacent 2NN sites are empty,  $N$  is the number of oxygen atoms adsorbed on adjacent 2NN sites surrounding the chemisorbing oxygen atoms,  $\Delta E$  is the change of adsorption activation energy due to  $\varepsilon_2$  repulsion between two oxygen atoms chemisorbed on adjacent 2NN sites. The dissociative chemisorption of the  $\text{O}_2$  molecules was simulated by Monte Carlo method on a  $200 \times 200$  square lattice of adsorption sites with periodic boundary conditions. The  $S$  value (at a certain oxygen surface coverage) is determined as the ratio between the number of  $\text{O}_2$  molecules dissociatively chemisorbed and the number of the Monte Carlo attempts of the adsorption of  $\text{O}_2$  molecules during some adsorption time. The model of the  $\text{O}_2$  chemisorption on a (100) metal surface and Monte Carlo algorithm are described in detail in [14,16].

## 3. Results and discussion

The simulations of the  $\text{O}_2$  chemisorption on a (100) surface by the Monte Carlo method according to this model show the dynamic picture of the formation of the  $p(2 \times 2)$  and  $c(2 \times 2)$  adsorption structures [16] observed during  $\text{O}_2$  chemisorption on (100) surfaces of metals [3–

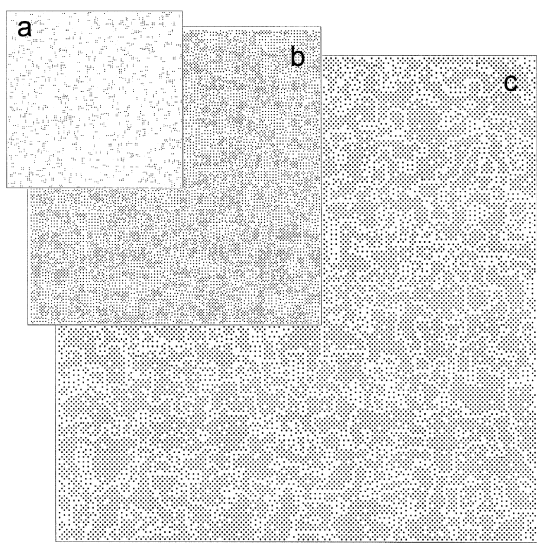


Fig. 1. Evolution in the adsorbed layer obtained by simulation of the  $O_2$  chemisorption on a  $200 \times 200$  square lattice at  $E_{\text{dir}} = 7$  kJ/mol,  $E_{\text{indir}} = 1$  kJ/mol,  $\Delta E = 1$  kJ/mol. The adsorbate coverages are (a)  $\sim 0.05$ , (b)  $\sim 0.28$  and (c)  $\sim 0.38$  ML. Chemisorbed oxygen atoms are presented as points; empty adsorption sites are not shown.

13]. The direct chemisorption pathway leads to the nucleation of adsorption islands, the indirect one to their growth. The  $p(2 \times 2)$  adsorption structure is nucleated at the beginning of chemisorption, whereas the  $c(2 \times 2)$  structure is formed later inside the  $p(2 \times 2)$  structure because the  $\varepsilon_2$  repulsion between atoms chemisorbed on 2NN sites decreases the probability of the formation of a fragment of the  $c(2 \times 2)$  structure. The ratio between the probabilities of the  $O_2$  adsorption via the direct and indirect pathways determine the character of the adsorption layer formation and the type of  $S(\theta)$  dependence. Langmuir adsorption with disordered  $p(2 \times 2)$  and  $c(2 \times 2)$  adsorption layers is observed if the direct adsorption predominates over the indirect one. Island-mediated adsorption with high degree of ordering in the  $p(2 \times 2)$  and  $c(2 \times 2)$  adsorption layers is observed when the indirect pathway predominates over the direct one [16].

A significant change in the character of the adsorption layer formation and type of  $S(\theta)$

dependence is observed at constant  $\Delta E$ ,  $E_{\text{indir}} = 1$  kJ/mol, and gradual increase of  $E_{\text{dir}}$  from 1 to 20 kJ/mol, i.e. at gradual change the effect of the direct and the indirect pathways on chemisorption.

Figs. 1 and 2 present the evolution in the adsorbed layer obtained by simulation of the  $O_2$  dissociative chemisorption at  $\Delta E$ ,  $E_{\text{indir}} = 1$  kJ/mol,  $E_{\text{dir}} = 7$  kJ/mol (Fig. 1) and 20 kJ/mol, Fig. 2. At  $E_{\text{dir}} = 1-7$  kJ/mol, a similar picture of the evolution in the adsorbed layer was observed during  $O_2$  chemisorption. So, at  $E_{\text{dir}} = 7$  kJ/mol, at the beginning of adsorption many small  $p(2 \times 2)$  islands nucleate (Fig. 1a). These islands grow to form a saturated disordered  $p(2 \times 2)$  layer in which a lot of small  $c(2 \times 2)$  islands are formed (Fig. 1b). At  $\theta > 0.3$ , during the saturation a completely disordered  $c(2 \times 2)$  layer are formed (Fig. 1c). At  $E_{\text{dir}} = 20$  kJ/mol, at the beginning of adsorption few  $p(2 \times 2)$  islands nucleate (Fig. 2a). Then they grow quickly to form an ordered  $p(2 \times 2)$  layer where the  $c(2 \times 2)$  islands nucleate (Fig. 2b).

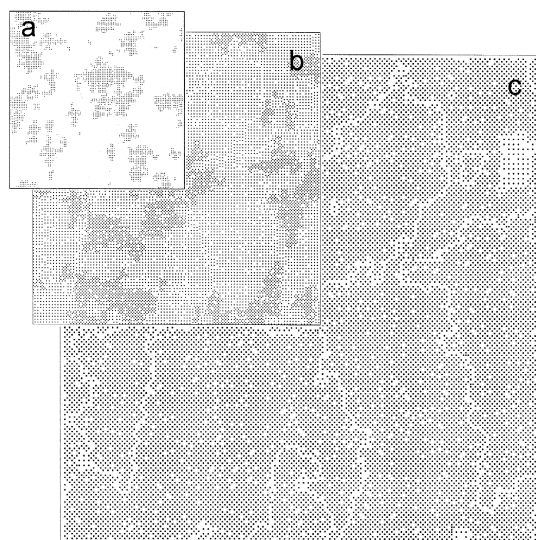


Fig. 2. Evolution in the adsorbed layer obtained by simulation of the  $O_2$  chemisorption on a  $200 \times 200$  square lattice at  $E_{\text{dir}} = 20$  kJ/mol,  $E_{\text{indir}} = 1$  kJ/mol,  $\Delta E = 1$  kJ/mol. The adsorbate coverages are (a)  $\sim 0.05$ , (b)  $\sim 0.28$  and (c)  $\sim 0.44$  ML. Chemisorbed oxygen atoms are presented as points; empty adsorption sites are not shown.

The growing  $c(2 \times 2)$  islands merge to form an ordered  $c(2 \times 2)$  layer at  $\theta > 0.4$  (Fig. 2c).

At  $E_{\text{dir}} = 1$  kJ/mol and  $\Delta E$ ,  $E_{\text{indir}} = 1$  kJ/mol, when both direct and indirect pathways are fast,  $S$  gradually decreases from  $S \sim 1.0$  at  $\theta \sim 0$  to  $S \sim 10^{-3}$  at  $\theta \sim 0.35$  (Fig. 3a(1)). Such character of the  $S(\theta)$  dependence is related to the fact that the direct adsorption pathway predominates over the indirect one at these  $E_{\text{dir}}$  and  $E_{\text{indir}}$  values. As a result, a lot of adsorption islands with  $p(2 \times 2)$  and  $c(2 \times 2)$  structures are formed at  $\theta \leq 0.2-0.25$  and  $\theta \geq 0.2-0.25$ , respectively. Meanwhile, the indirect pathway does not provide their significant growth. So, small islands merge to form a saturated disordered adsorption layer with  $p(2 \times 2)$

and  $c(2 \times 2)$  structures at  $\theta \sim 0.2-0.25$  and  $\theta \sim 0.35-0.4$ , respectively.

At  $\Delta E$ ,  $E_{\text{indir}} = 1$  kJ/mol,  $S_0$  decreases as  $E_{\text{dir}}$  grows from 1 to 7 kJ/mol, and the beginning part of  $S(\theta)$  dependence drops because the nucleation probability of the  $p(2 \times 2)$  adsorption islands decreases. Therefore, their concentration and the overall adsorption rate also become lower. At  $E_{\text{dir}} = 7$  kJ/mol, a constant value  $S \sim 0.1$  is observed at  $\theta \leq 0.15$  (Fig. 3a(2)) as the gradual decrease of the direct adsorption rate is compensated by a gradual increase of the contribution of the indirect pathway in chemisorption with the coverage growth. As a result, there are many small adsorption islands with the  $p(2 \times 2)$  structure on the surface at  $\theta \sim 0.05$  (Fig. 1a). At  $\theta \geq 0.15$ , a fast drop of  $S$  is observed (Fig. 3a(2)) due to the saturation of the  $p(2 \times 2)$  layer where the adsorption rate is significantly lower due the effect of  $\varepsilon_2$  repulsion. So, at  $\theta \sim 0.28$ , many small  $c(2 \times 2)$  islands are observed (Fig. 1b). As a result of the merging of these islands, a disordered  $c(2 \times 2)$  layer is formed at  $\theta \sim 0.38$  (Fig. 1c).

At  $\Delta E$ ,  $E_{\text{indir}} = 1$  kJ/mol and  $E_{\text{dir}} > 7$  kJ/mol, the character of the  $S(\theta)$  dependence is substantially different. At the beginning of adsorption at  $\theta = 0-0.05$ ,  $S$  increases with the  $\theta$  growth. At  $\theta = 0.05-0.15$ ,  $S$  reaches maximum level and drops fast at  $\theta > 0.15$ . Then at  $\theta \geq 0.2$ ,  $S$  is almost constant and drops again after the saturation of the  $c(2 \times 2)$  layer. Such character of the  $S(\theta)$  dependence is related to the notable domination of the indirect pathway over the direct one at  $E_{\text{dir}} > 7$  kJ/mol and  $E_{\text{indir}} = 1$  kJ/mol. At these  $E_{\text{dir,indir}}$  values, at the beginning of the adsorption ( $\theta < 0.15$ ), the  $p(2 \times 2)$  adsorption islands nucleate slowly, and their concentration is low enough to provide their significant growth prior the merge via the indirect pathway. So, the contribution of the indirect pathway in chemisorption gradually increases resulting in an increase of the adsorption rate with the  $\theta$  growth. At  $\theta \geq 0.15$ , the  $p(2 \times 2)$  islands start to merge, i.e. the  $p(2 \times 2)$  layer is saturated, and  $c(2 \times 2)$  layer begins to form. As

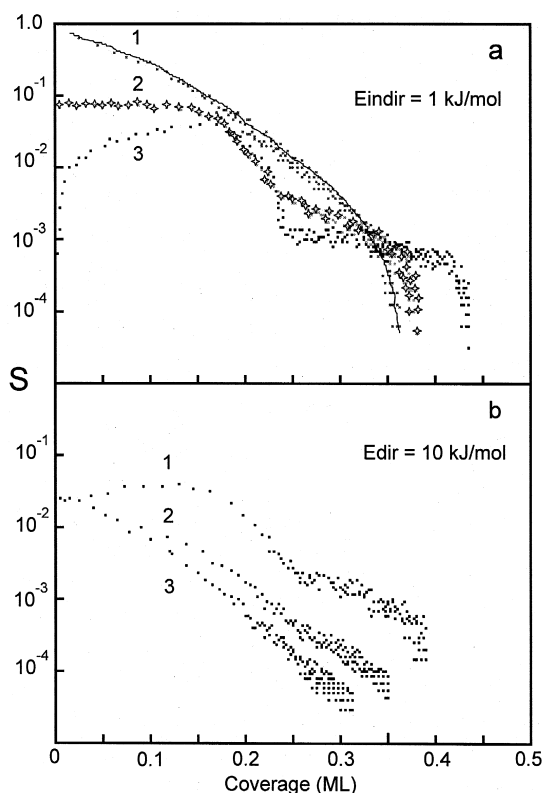


Fig. 3.  $S(\theta)$  dependencies obtained by simulation of the  $O_2$  chemisorption on a  $200 \times 200$  square lattice: (a)  $\Delta E$ ,  $E_{\text{indir}} = 1$  kJ/mol,  $E_{\text{dir}} = 1$  kJ/mol (1), 7 kJ/mol (2) and 20 kJ/mol (3); (b)  $\Delta E = 1$  kJ/mol,  $E_{\text{dir}} = 10$  kJ/mol,  $E_{\text{indir}} = 1$  kJ/mol (1), 7 kJ/mol (2) and 20 kJ/mol (3).

a result, the adsorption rate decreases. The subsequent behavior of the  $S(\theta)$  dependence is related to the formation of the  $c(2 \times 2)$  layer.

At  $E_{\text{dir}} = 20$  kJ/mol ( $\Delta E$ ,  $E_{\text{indir}} = 1$  kJ/mol), i.e. under conditions when the growth of the adsorption islands dominates over their nucleation, there are two distinct areas on the  $S(\theta)$  curve related to the formation of the  $p(2 \times 2)$  at  $\theta \leq 0.2-0.25$  and  $c(2 \times 2)$  layer at  $\theta \geq 0.2-0.25$  (Fig. 3a(3)). The  $p(2 \times 2)$  adsorption layer is formed by the nucleation of  $p(2 \times 2)$  islands via the slow direct adsorption pathway and their gradual growth via the fast indirect one. As a result,  $S(\theta)$  increases at low coverage (Fig. 3a(3)) and large  $p(2 \times 2)$  islands are formed on the surface at  $\theta \sim 0.05$  (Fig. 2a). The  $c(2 \times 2)$  adsorption layer is slowly formed by nucleation and growth of  $c(2 \times 2)$  adsorption islands during the saturation of the  $p(2 \times 2)$  layer, because the repulsion between the particles adsorbed on neighboring 2NN sites decreases the probability of chemisorption significantly. The  $c(2 \times 2)$  islands are mostly formed by the merge of the antiphase  $p(2 \times 2)$  islands spatially not coherent with respect to each other in both directions, and grow due to the indirect chemisorption [16]. Direct adsorption inside the  $p(2 \times 2)$  layer is hardly possible because the effect of the repulsive lateral environment from atoms chemisorbed on adjacent 2NN sites is high under these conditions. Therefore, a constant  $S$  value is observed during the formation of the  $c(2 \times 2)$  layer at  $0.25 < \theta < 0.45$  (Fig. 3a(3)) and few  $c(2 \times 2)$  islands are formed at  $\theta \sim 0.28$  (Fig. 2b). A sharp  $S$  decrease is observed only at  $\theta \sim 0.45$  due to the decrease in number of empty neighbor 3NN adsorption sites required for the dissociative oxygen chemisorption in a more ordered saturated adsorption layer (Fig. 2c).

The decrease of the contribution of indirect adsorption in chemisorption ( $E_{\text{indir}} = 1, 7, 20$  kJ/mol) at constant  $E_{\text{dir}} = 10$  kJ/mol results in a gradual lowering of the whole  $S(\theta)$  dependence (Fig. 3b). The effect of direct adsorption on chemisorption is increased with the  $E_{\text{indir}}$

growth from 1 to 20 kJ/mol. Therefore, the concentration of the adsorption islands grows while their size prior to the merge decreases. This results in disordering of the  $p(2 \times 2)$  and  $c(2 \times 2)$  adsorption layers.

#### 4. Conclusion

The simulation of the  $O_2$  chemisorption on a (100) metal surface by Monte Carlo method on the basis of a model that takes into account the direct and indirect adsorption pathways and repulsive lateral interactions in the adsorption layer indicate that the formation of the  $p(2 \times 2)$  and  $c(2 \times 2)$  adsorption structures have a significant effect on the character of the adsorption layer formation and type of  $S(\theta)$  dependence. The ratio between the activation energy of adsorption via the direct and indirect pathways (at  $E_{\text{dir,indir}} = 1-20$  kJ/mol) determines the average concentration of the adsorption islands and their average size prior to the merge, which determine the degree of ordering in the saturated layer with  $p(2 \times 2)$  and  $c(2 \times 2)$  structures. If the direct adsorption pathway predominates over the indirect one ( $E_{\text{dir}}/E_{\text{indir}} < 7-8$ ), many adsorption islands nucleate, while the indirect pathway does not provide significant growth of the islands. So, they merge to form disordered  $p(2 \times 2)$  and  $c(2 \times 2)$  adsorption layers, i.e. Langmuir adsorption when  $S$  decreases as  $\theta$  grows is observed. At  $E_{\text{dir}}/E_{\text{indir}} \sim 7$ , a constant  $S$  value is observed at the beginning of adsorption, because during the adsorption the lowering of the direct pathway contribution in chemisorption is compensated by an increase of the effect of the indirect pathway on chemisorption. If the indirect adsorption pathway predominates over the direct one ( $E_{\text{dir}}/E_{\text{indir}} > 7-8$ ), the adsorption islands nucleate slowly while faster indirect adsorption provides their significant growth prior to the merge. As a result, the effect of the indirect pathway on chemisorption is increased with the  $\theta$  growth, thus accelerating the adsorption. In this case, the slow nucleation and fast

growth of the adsorption islands are observed, and  $S(\theta)$  dependence passes over a maximum. Thus, complex structural transformations in oxygen adsorption layer during the  $O_2$  chemisorption on (100) metal surfaces have a significant effect on the oxygen adsorption rate.

## Acknowledgements

This work was supported by the Russian Foundation for Basic Research, grant 99-03-32429.

## References

- [1] M.A. Morris, M. Bowker, D.A. King, in: C.H. Bamford, C.F.H. Tipper, R.G. Compton (Eds.), *Comprehensive Chemical Kinetics, Simple Processes at the Gas–Solid Interface* Vol. 19 Elsevier, Amsterdam, 1984, p. 55.
- [2] D.G. Castner, G.A. Somorjai, *Chem. Rev.* 79 (1979) 233.
- [3] G. Ertl, J. Koch, *Z. Phys. Chem* 69 (1970) 323.
- [4] E.M. Stuve, R.J. Madix, C.R. Brundle, *Surf. Sci.* 146 (1984) 155.
- [5] T.W. Orent, S.D. Bader, *Surf. Sci* 115 (1982) 323.
- [6] S.L. Chang, P.A. Thiel, J.W. Evans, *Surf. Sci.* 205 (1988) 117.
- [7] S.L. Chang, P.A. Thiel, *J. Chem. Phys* 88 (1988) 2071.
- [8] D.G. Castner, B.A. Sexton, G.A. Somorjai, *Surf. Sci.* 71 (1978) 519.
- [9] J.R. Mercer, P. Finetti, F.M. Leibsle, R. McGrath, V.R. Dhanak, A. Baraldi, K.C. Prince, R. Rosei, *Surf. Sci.* 352–354 (1996) 173.
- [10] W. Oed, B. Dotsch, L. Hammer, K. Heinz, K. Muller, *Surf. Sci.* 207 (1988) 55.
- [11] G.B. Fisher, S.J. Schmieg, *J. Vac. Sci. Technol. A* 1 (1983) 1064.
- [12] P.H. Holloway, J.B. Hudson, *Surf. Sci.* 43 (1974) 123.
- [13] C.R. Brundl, J.Q. Broughton, in: D.A. King, D.P. Woodruff (Eds.), *Chemisorption Systems, Part A. The Chemical Physics of Solid Surface and Heterogeneous Catalysis* Vol. 3A Elsevier, Amsterdam, 1990, p. 268.
- [14] A.N. Salanov, V.N. Bibin, N.A. Rudina, *React. Kinet. Catal. Lett.* 64 (1998) 261.
- [15] A.N. Salanov, V.N. Bibin, N.A. Rudina, *React. Kinet. Catal. Lett.* 64 (1998) 269.
- [16] A.N. Salanov, V.N. Bibin, *Surf. Sci.* 441 (1999) 399.
- [17] *Kinetics of Interface Reactions*, Springer Series in Surface Sciences, M. Grunze, H.J. Kreuzer (Eds.), Part II. Precursors: Myth or Reality? Vol. 8 Springer-Verlag, Berlin, 1987, p. 94.
- [18] C.R. Brundle, J. Behm, J.A. Barker, *J. Vac. Sci. Technol., A* 2 (1984) 1038.
- [19] C.R. Brundle, *J. Vac. Sci. Technol., A* 3 (1985) 1468.
- [20] M.I. Temkin, *Zh. Fiz. Khim.* (Russia) 15 (1941) 296.
- [21] M.I. Temkin, *Adv. Catal.* 28 (1979) 173.